

# Measuring the time and scale-dependency of subaerial rock weathering rates over geologic time scales with ground-based lidar

Amit Mushkin<sup>1,2</sup>, Amir Sagy<sup>1</sup>, Eran Trabelci<sup>1,3</sup>, Rivka Amit<sup>1</sup>, and Naomi Porat<sup>1</sup>

<sup>1</sup>Geological Survey of Israel, 30 Malkhe Israel Street, Jerusalem 95501, Israel

<sup>2</sup>University of Washington, 1410 NE Campus Parkway, Seattle, Washington 98195, USA

<sup>3</sup>Hebrew University in Jerusalem, Givat Ram, Jerusalem 91904, Israel

## ABSTRACT

The evolution of roughness as a function of surface age was used to quantify weathering rates on rocky desert surfaces. Surface topography on eight late Quaternary alluvial terraces, which record the weathering of Holocene ( $5 \pm 1$  ka) boulder-strewn deposits into mature ( $87 \pm 2$  ka) desert pavements in the Negev desert of Israel, was measured with ground-based lidar. Roughness on each terrace was characterized with power spectral density (PSD) analysis, and changes in PSD as a function of length scale ( $\lambda \sim 0.04$ – $1.50$  m) and surface age were used to estimate diminution/weathering rates of the surface rocks. We found PSD values that systematically increase as a power-law function of  $\lambda$  (roughness exponent of  $\sim 2.0$ ) and decrease as an inverse power-law function of surface age. This PSD evolution indicates a fragmentation rock weathering process driven by salt shattering throughout the 87 k.y. period examined. PSD analysis of the lidar data also revealed weathering rates that increase with rock size and decrease as an inverse power-law function of time, from initial values  $>20$  mm/k.y. to  $<1$  mm/k.y. within  $\sim 60$  k.y.

## INTRODUCTION

Weathering and conversion of rock into regolith are fundamental surface processes on Earth and other terrestrial planets such as Mars. Efforts to quantify these processes and their rates remain key aspects in the ongoing push to better understand the role of weathering in landscape evolution over geologic time scales (e.g., Larsen et al., 2014). In desert environments, subaerial rock weathering is one of the principal processes driving the evolution of otherwise stable rocky surfaces. Process-oriented studies indicate that the rates of such weathering decrease nonlinearly over geologic time scales (Colman, 1981; Crook and Gillespie, 1986; Amit et al., 1993). And yet, quantitative estimates for subaerial rock weathering rates are commonly reported as time-averaged constants derived from interpretation of cosmogenic radionuclide measurements with constant-rate surface erosion models (e.g., Matmon et al., 2009; Portenga and Bierman, 2011). Here, to address our limited ability to quantify rock weathering rates that change over geologic time scales, we examine the smoothing of progressively weathered rocky surfaces over Quaternary time scales as a new approach for measuring time-variant rock weathering rates.

Our approach is based on high-resolution three-dimensional (3-D) lidar scanning of surface topography (Fig. 1) and on scale-dependent (spectral) analysis of roughness and its evolution as a function of surface age (Figs. 2 and 3). We focus on a suite of eight abandoned alluvial terraces in the hyperarid Negev desert of Israel ( $87$ – $5$  ka; Table 1) and are able for the first time to estimate subaerial rock weathering rates on such landforms as time-variant functions rather than as time-averaged constants.

## BACKGROUND AND METHODS

Rock-surface roughness has been previously suggested as an indicator for the degree of rock weathering (e.g., McCarroll and Nesje, 1996). Here we expand on this and examine changes in roughness (i.e., smoothing) of rocky landforms over geologic time scales as an effective statistical measure for weathering rates of rock populations. We focus on desert alluvial chronosequences composed of mappable successions of progressively weathered rock-dominated deposits, which typically record the post-abandonment weathering of young and rough boulder-strewn deposits into smooth and persistent desert pavements (Amit and Gerson, 1986; McFadden et al., 1987, 1989; Wells et al., 1995). Previous studies examined desert chronosequences and/or desert pavements primarily in the context of inferring past climatic, tectonic, and environmental conditions (Wells et al., 1987; Amit et al., 1996; Quade, 2001; Matmon et al., 2009). Here we examine the roughness of such land-

forms in order to infer the weathering history of their surface rocks.

Roughness is a scale-dependent property of natural surfaces often analyzed using Fourier transformation of topographic data. The Fourier transform offers an effective statistical measure for quantifying the scaling of roughness (expressed in terms of power spectral density, PSD) as a function of length scale (expressed in terms of wavelength or spatial frequency) (Brown and Scholz, 1985). Accordingly, PSD analysis is routinely used to identify and examine roughness components of geologic surfaces (e.g., Gilbert, 1989; Turcotte, 1997; Perron et al., 2008).

PSD analysis of topographic profiles spanning length scales of  $10^{-3}$ – $10^1$  m across Holocene alluvial deposits in Death Valley, California (USA), was previously used to demonstrate the self-affine roughness characteristics of such gravel- to boulder-dominated surfaces at length scales of less than several meters (Weeks et al., 1996). Here we examine the evolution of PSD and roughness of such surfaces over Quaternary time scales as they weather and mature into smooth gravel-armored desert pavements.

## Field Sites and Surface Ages

The two studied alluvial fans are located within the Arava valley segment of the Dead Sea Transform (Fig. 1). Similar in area ( $\sim 20$  km<sup>2</sup>) and catchment size ( $\sim 150$  km<sup>2</sup>), both the Shehoret and Raham fans extend  $\sim 5$  km eastward from the mountain front into the valley floor Evrona playa. Both fans have been affected by tectonic base-level lowering, resulting in channel incision and sequential abandonment

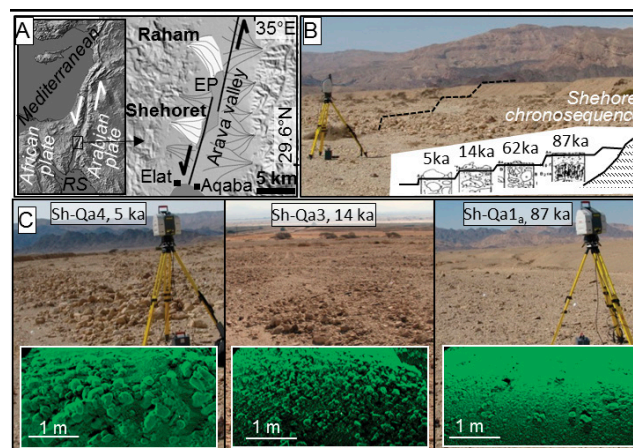


**Figure 1.** A: Study area (black box) within the Arava valley segment of the Dead Sea Transform (DST) separating the African and Arabian plates. RS—Red Sea, EP—Evrona playa. B: Top shows the Shehoret chronosequence; bottom shows a generalized cross section of the main terraces examined. Soil profile illustrations are from Amit et al. (1993). C: Shehoret terraces (top) and point-cloud rendering of their respective lidar scans (62 ka terrace not shown).

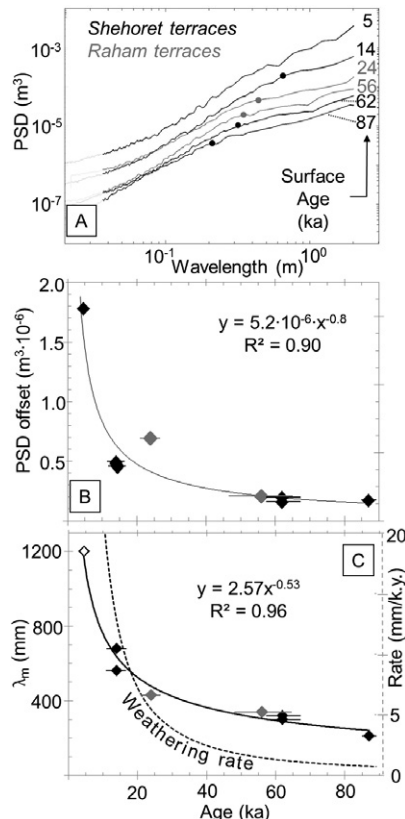


**Figure 2. A:** Power spectral density (PSD) curves for the studied terraces. Surface abandonment ages are listed on the right. Solid dots mark the slope breakpoint for each curve (see Item DR2 [see footnote 1] for further details). Two additional PSD curves from the 14 ka and 62 ka surfaces are not shown, as they largely overlap the presented curves for these terraces. **B:** Power-law decrease of PSD offset as a function of surface age indicating time-variant smoothing rates. **C:** Power-law decrease in  $\lambda_m$  (length scale of PSD slope breakpoint) as a function of surface age (solid line). Dashed line (the slope of the  $\lambda_m$  versus surface age power-law function) describes the decrease in maximum rock weathering rates on the examined surfaces. Horizontal bars in B and C represent age uncertainties. Open diamond in C is a minimum value (upper limit of measurement scale), as the 5 ka surface does not display a breakpoint in PSD slope.

of terraces (Amit et al., 1996). The abandoned terraces form well-preserved chronosequences due to the persistent hyperaridity of this region throughout the Quaternary (Amit et al., 2006).

The terraces examined at both chronosequences share a common lithological assemblage dominated by Phanerozoic carbonates, up to ~15% Precambrian magmatics, and trace amounts of sandstones. At Shehoret, soil profiles indicate time-invariant fluvial deposition characteristics (Amit et al., 1996; Fig. DR1 in the GSA Data Repository<sup>1</sup>) and simple

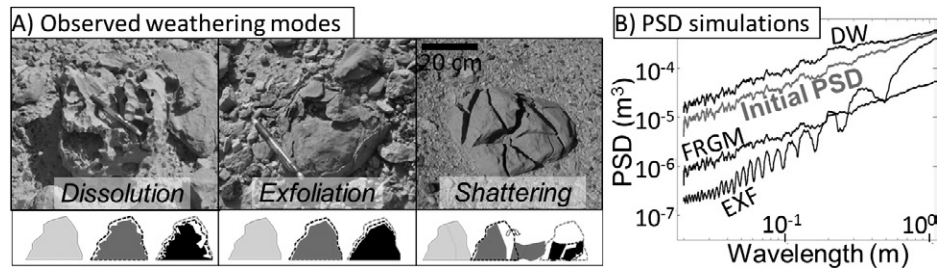


**Figure 3. A:** Rock weathering modes observed on the studied surfaces and illustration of their evolution through time from fresh (gray) to progressively weathered products (black). **B:** Simulated power spectral density (PSD) evolution in which the weathering modes drive distinguishable PSD evolution trends (gray is initial synthetic surface, black is simulation results). Dissolution weathering (DW) was simulated by numerical addition of high-frequency roughness to the initial surface. Exfoliation (EXF) was simulated by numerical smoothing of high-frequency roughness (increased noise level is a numerical artifact). Clast shattering was simulated through scale-invariant fragmentation (FRGM).

TABLE 1. SURFACE CHARACTERISTICS OF EXAMINED TERRACES

| Terrace                          | Geomorphic surface description   | Lidar scan location      | Scanned area (m <sup>2</sup> ) | PSD slope*  | PSD offset <sup>†</sup> (m <sup>2</sup> · 10 <sup>-7</sup> ) | PSD slope breakpoint [ $\lambda_m$ (m), log PSD] |
|----------------------------------|--|--------------------------|--------------------------------|-------------|--|--|
| Sh-Qa4<br>5 ± 1 ka               | gravels to boulders, rounded, weakly varnished, prominent bar and swale morphology   | 29°36.932N<br>34°58.292E | 21                             | 1.84 ± 0.02 | 17.78  | –  |
| Sh-Qa3<br>14 ± 2 ka              | gravels to boulders, rounded to angular, completely varnished, remnant bar and swale morphology, poorly developed pavement | 29°36.867N<br>34°58.503E | 37                             | 2.08 ± 0.01 | 4.90   | (0.56, –4.11)                                    |
| Sh-Qa1 <sub>b</sub><br>62 ± 5 ka | gravels, angular, heavily varnished, no bar and swale morphology, well-developed pavement                                  | 29°36.679N<br>34°59.168E | 20 <sup>§</sup>                | 2.18 ± 0.02 | 4.79   | (0.68, –3.71)                                    |
|                                  |  | 29°37.030N<br>34°58.223E | 33 <sup>§</sup>                | 2.11 ± 0.01 | 1.55   | (0.30, –5.04)                                    |
| Sh-Qa1 <sub>a</sub><br>87 ± 2 ka | gravels, angular, heavily varnished, no bar and swale morphology, very well-developed pavement                             | 29°36.596N<br>34°58.486E | 44                             | 1.98 ± 0.01 | 1.91   | (0.32, –4.95)                                    |
|                                  |  | 29°36.374N<br>34°58.543E | 20                             | 1.93 ± 0.02 | 1.7  | (0.21, –5.45)                                    |
| Ra-Q2<br>24 ± 3 ka               | gravels to boulders, rounded to angular, completely varnished, remnant bar and swale morphology, fairly developed pavement | 29°42.165N<br>35°00.177E | 50                             | 1.73 ± 0.02 | 6.92   | (0.43, –4.37)                                    |
| Ra-Q1<br>56 ± 10 ka              | gravels, angular, heavily varnished, no bar and swale morphology, well-developed pavement                                  | 29°42.980N<br>34°59.403E | 31                             | 2.21 ± 0.02 | 2.04   | (0.34, –4.68)                                    |

Note: Sh—Shehoret, Ra—Raham. Lidar—light detection and ranging. PSD—power spectral density.

\*R<sup>2</sup> > 0.98 for all log-log linear regressions.

<sup>†</sup>PSD value of linear regression at  $\lambda = 10^{-1.35}$  m. Uncertainty <1% for all surfaces.

<sup>§</sup>PSD curve is not displayed in Figure 2A for clarity.

postabandonment Reg soil development void of burial and/or exhumation (resurfacing) events (Table DR1 in the Data Repository). Consistent with their soil evolution, surface weathering indices such as rock varnish development, magnitude of bar-swale relief, and size-frequency distribution of surface rocks (Fig. DR1) also indicate progressive weathering with increasing age (Table 1). Shattering by salts (Amit et al., 1993), dissolution weathering (indicated by ubiquitous pitting on rock surfaces), and exfoliation (to a lesser degree)

appear to be the primary drivers of rock weathering on the examined surfaces.

Age estimates for terrace abandonment are based on luminescence measurements from the uppermost deposits in each terrace (see Porat et al., 2010, for details). At Shehoret, we focused on 4 terraces with abandonment ages of 5 ± 1 ka, 14 ± 2 ka, 62 ± 5 ka, and 87 ± 2 ka (Porat et al., 2010), and at the Raham site (Crouvi et al., 2006) we focused on 2 terraces with abandonment ages of 24 ± 3 ka and 56 ± 10 ka (Item DR1 in the Data Repository).

<sup>1</sup>GSA Data Repository item 2014366, lidar scanning and luminescence dating at the Raham chronosequence, and definition of slope breakpoint, is available online at [www.geosociety.org/pubs/ft2014.htm](http://www.geosociety.org/pubs/ft2014.htm), or on request from [editing@geosociety.org](mailto:editing@geosociety.org) or Documents Secretary, GSA, P.O. Box 9140, Boulder, CO 80301, USA.

## Lidar Scanning and Data Processing

Lidar scanning was carried out with a Leica ScanStation 2 ground-based unit. Detailed field mapping preceded selection of 20–50 m<sup>2</sup> areas capturing the roughness variability of each terrace. Scans were typically executed at 5 mm resolution (ground sampling distance) and were limited to within bars in cases where bar and swale morphology was present. Each area was scanned from three to four different view angles to reduce the inherent problem of occlusions on rough surfaces. Subscans were then coregistered into a single point cloud (registration uncertainties of <4 mm), which was then interpolated into an evenly spaced topographic grid with typical resolution of ~5 mm/pixel. PSD for wavelengths between 0.04 and 1.5 m was then calculated for hundreds of parallel profiles on each surface (Brodsky et al., 2011), and in all cases were found to be independent of profile orientation.

The time-progressive smoothing of desert pavement over Quaternary time scales is typically driven by (1) reduction of surface rock size through subaerial weathering (Wells et al., 1995); (2) gravity-driven diffusion from bars into swales (Matmon et al., 2009; Frankel and Dolan, 2007; Regmi et al., 2014); and (3) eolian deposition of fines and their accumulation as a clast-free Av horizon beneath the pavement rocks (McFadden et al., 1987). However, because our lidar data were acquired only within bars and the pavement rocks characteristically “float” on top of their underlying Av horizon (Fig. DR2), the effect of the latter two processes on our lidar measurements and PSD analysis is expected to be minor. Thus, our results primarily relate to the in-situ weathering/diminution process of surface rocks on the examined terraces.

## RESULTS

PSD values for the terraces of both chronosequences systematically increase as a function of wavelength ( $\lambda = 0.04$ –1.50 m) and decrease as a function of surface age ( $t$ , 87–5 ka) (Fig. 2A). In physical terms, this PSD- $\lambda$  relation reflects the increasing relief encountered on each surface as measurement length scale is increased (e.g., boulder-dominated relief sampled at 1 m wavelengths is greater than gravel-dominated relief sampled at 0.05 m wavelengths). The PSD decrease with time reflects the time-progressive smoothing of the surfaces. This measured PSD evolution is also consistent with conventional rock counts (Fig. DR1) that reveal gradually varying size-frequency distribution curves for each surface and overall rock size diminution with increasing surface age.

The youngest terrace (5 ka) displays a linear PSD curve in log-log space (Fig. 2A) similar to the PSD curves of the self-affine Holocene terraces in Death Valley, California (Weeks et al., 1996). We therefore suggest that PSD values for

the 5 ka surface in Figure 2A can be approximated as a power-law function of  $\lambda$ :

$$\text{PSD} = C \cdot \lambda^\alpha, \quad (1)$$

where  $\alpha$  is the slope (roughness exponent) and  $C$  is the offset term of this function in log-log space (Fig. 2A). The older terraces we examined display bilinear PSD curves with a sharp transition point (breakpoint) to a moderated slope at longer wavelengths. Below the wavelength ( $\lambda_m$ ) of their respective breakpoints, all terraces display similarly sloping linear PSD curves with an approximate time-invariant roughness exponent of  $2.01 \pm 0.17$ , and an offset term that monotonically decreases as a function of surface age (Table 1; Fig. 2B). Thus, we regard  $C$ , which is expected to vary with surface RMS (root mean square) (Weeks et al., 1996), as the primary time-dependent variable in this system. In physical terms, such PSD evolution implies that, as the terrace surfaces smooth over time, the scaling of their roughness with  $\lambda$  does not significantly change for  $\lambda < \lambda_m$ .

Plotting  $C$  for each curve in Figure 2A versus surface age reveals an inverse power-law relation between these two independent surface attributes (Fig. 2B):

$$C = c_1 \cdot t^{-c_2}, \quad (2)$$

where  $c_1$  and  $c_2$  are time-invariant constants that can be empirically determined from the regression in Figure 2B. Inserting Equation 2 into Equation 1, we obtain:

$$\text{PSD} = 5.2 \cdot 10^{-6} \cdot t^{-0.8} \cdot \lambda^{2.01}, \quad (3)$$

which provides a first-order approximation for PSD evolution in this system for  $\lambda < \lambda_m$  and  $5 < t < 87$  ka. Thus, Equation 3, which primarily applies to the in-situ weathering/diminution of surface rocks, indicates scale-dependent rock weathering rates that increase as a function of  $\lambda$  (i.e., rock size) and asymptotically decrease as a function of time.

## DISCUSSION

### Time-Variant Weathering Rates

Straightforward translation of PSD decrease through time into physical rock weathering rates as commonly examined in terms of mm/k.y. is not trivial because smoothing is scale dependent (Equation 3) and PSD is a mathematical term strictly applicable to the statistical representation of roughness through the Fourier transform. To address these complexities, we focus on the PSD slope moderation at longer wavelengths (Fig. 2A), which reflects the paucity in topographic variations beyond the length scale of the largest rocks present on the surface (Fig. DR1). Thus, regarding  $\lambda_m$  as the effective length scale of the largest rocks on each terrace, we plot  $\lambda_m$  (in mm) as a function of surface age (in ka) (Fig. 2C) and use the slope of this function to constrain maximum rock weathering/diminution rates (in mm/k.y.) as a function of time. Our results reveal a power-law decrease in rock weathering

rates from initial values of >20 mm/k.y. down to <1 mm/k.y. within a period of ~60 k.y.

Persistent Quaternary hyperarid conditions in our study area (Amit et al., 2006) suggest that the power-law decrease in weathering rates indicated in Figure 2C reflects an inherent property of the weathering process (discussed in the following) rather than changes in the environmental conditions driving it. Thus, while time-variant rock weathering rates have been previously inferred in desert environments, based on crack density in surface rocks (Crook and Gillespie, 1986) and measurements of percent shattered clasts (Amit et al., 1993), our results provide the first quantification of such time-variant rock weathering rates in terms of millimeters per year.

In the context of cosmogenic radionuclides, high initial weathering rates that rapidly decrease imply that the shielding of a surface sample would be overestimated if a constant-rate erosion model is employed. Accordingly, we propose that time-variant weathering rate functions (e.g., Fig. 2C), which can support quantitative time-variant surface evolution models, may also help improve our ability to interpret cosmogenic radionuclide measurements from weathered rocky surfaces.

### Weathering Processes

Dissolution weathering, exfoliation, and salt shattering all appear to contribute to rock diminution on the studied surfaces (Fig. 3A). We examined whether roughness data can be used to spectrally distinguish between these different weathering processes (Fig. 3B). Dissolution weathering, which is typically manifested by high-frequency pitting of rock surfaces that increases roughness at the centimeter to decimeter length scales, is expected to yield a decrease in PSD slope with time as roughness is added to the system at shorter wavelengths through pitting. In contrast, exfoliation, which is typically manifested by smoothing of high-frequency roughness elements, is expected to yield an increase in PSD slope with time as shorter wavelength elements are more effectively removed from rock surfaces. However, shattering of rocks through scale-invariant fragmentation, which is assumed to result in a fractal distribution (Turcotte, 1997; Perfect, 1997), would be expected to yield time-invariant PSD slopes (roughness exponents) as PSD at all length scales is reduced by a common factor.

Thus, the approximate time-invariant roughness exponents of the PSD curves in Figure 2A (for  $\lambda < \lambda_m$ ) point toward rock shattering by salts as the dominant weathering process throughout the 87 k.y. period examined. In addition, the fragmentation nature of rock diminution on the studied surfaces indicates that rock shattering by salts, in the case examined here, is a scale-invariant process (at  $\lambda > 0.04$  m) over geologic time scales. In a wider context, we propose that the roughness-for-weathering approach presented here also offers unique and

quantitative field-based inputs to the ongoing debate regarding the cracking of surface clasts on desert surfaces through physical drivers such as differential moisture retention (Moore et al., 2008), directional insolation (McFadden et al., 2005; Eppes et al., 2010), and/or salt weathering (Yaalon, 1970; Amit et al., 1993).

### Applicability to Other Rocky Terrains

Previous studies determined that conventional statistical measures for surface rock populations, such as maximum size and/or the mean, were insufficient for inferring the age of late Quaternary alluvial units, although age-progressive rock size diminution was apparent in the field (McFadden et al., 1989; Frankel and Dolan, 2007). Our results suggest that this apparent discrepancy may result in part from scale-dependent rock weathering (in terms of mm/k.y.) and non-normal size-frequency distribution of rocks (Fig. DR1). In contrast, the systematic behavior we find for PSD as a function of surface age (Fig. 2A) indicates that spectral description of roughness may be more adequate for quantifying time-progressive rock size diminution on desert alluvial surfaces. Thus, our results indicate that with proper calibration, PSD analysis of lidar measurements at length scales of less than several meters can also be utilized as quantitative proxies for the age of desert alluvial surfaces.

The roughness-for-weathering approach is also applicable to alluvial sequences with other lithologies as well as additional rocky landforms such as pediments, hamada surfaces, glacially striated outcrops, glacial deposits, avalanche piles, and rock slides. Accordingly, spectral analysis of topography changes through time offers a new and readily applicable tool for quantifying sub-aerial rock weathering processes and their rates across a wide variety of settings.

### Broader-Scale Implications

Our ability to measure the topography of natural terrains at millimeter scales and above is greatly improving with the rapid development of 3-D surveying technologies such as lidar and/or automated photogrammetry. In this broad framework, we propose that roughness evolution over time (determined with repeat measurements or with space-for-time substitution; e.g., this study) is becoming a measurable characteristic of geomorphic surface processes that can be used to better inform our models of landscape evolution over geologic time scales.

### ACKNOWLEDGMENTS

The code for generation of power spectral density was written by E. Brodsky. The code for generation of synthetic surfaces was written by R. Toussaint. We thank G. Hetz for his assistance in the field and M. Eppes and three anonymous reviewers for their comments, which greatly helped improve the clarity of the manuscript. This research was funded by Israel Science Foundation (ISF) grant 12206/09.

### REFERENCES CITED

- Amit, R., and Gerson, R., 1986, The evolution of Holocene Reg (gravelly) soils in deserts: an example from the Dead Sea region: *Catena*, v. 13, p. 59–79, doi:10.1016/S0341-8162(86)80005-4.
- Amit, R., Gerson, R., and Yaalon, D., 1993, Stages and rate of the gravel shattering process by salts in desert Reg soils: *Geoderma*, v. 57, p. 295–324, doi:10.1016/0016-7061(93)90011-9.
- Amit, R., Harrison, J.B.J., Enzel, Y., and Porat, N., 1996, Soils as a tool for estimating ages of Quaternary fault scarps in a hyperarid environment—The southern Arava valley, the Dead Sea Rift, Israel: *Catena*, v. 28, p. 21–45, doi:10.1016/S0341-8162(96)00028-8.
- Amit, R., Enzel, Y., and Sharon, D., 2006, Permanent Quaternary hyperaridity in the Negev, Israel, resulting from regional tectonics blocking Mediterranean frontal systems: *Geology*, v. 34, p. 509–512, doi:10.1130/G22354.1.
- Brodsky, E.E., Gilchrist, J.J., Sagi, A., and Colletini, C., 2011, Faults smooth gradually as a function of slip: *Earth and Planetary Science Letters*, v. 302, p. 185–193, doi:10.1016/j.epsl.2010.12.010.
- Brown, S.R., and Scholz, C.H., 1985, Broad bandwidth study of the topography of natural rock surfaces: *Journal of Geophysical Research*, v. 90, p. 2575–2582, doi:10.1029/JB090iB14p12575.
- Colman, S.M., 1981, Rock-weathering rates as functions of time: *Quaternary Research*, v. 15, p. 250–264, doi:10.1016/0033-5894(81)90029-6.
- Crook, R., Jr., and Gillespie, A.R., 1986, Weathering rates in granitic boulders measured by P-wave speeds, in Colman, S.M., and Dethier, D., eds., *Rates of chemical weathering of rocks and minerals*: New York, Academic Press, p. 395–417.
- Crouvi, O., Ben-Dor, E., Beyth, M., Avigad, D., and Amit, R., 2006, Quantitative mapping of arid alluvial fan surfaces using field spectrometer and hyperspectral remote sensing: *Remote Sensing of Environment*, v. 104, p. 103–117, doi:10.1016/j.rse.2006.05.004.
- Eppes, M.C., McFadden, L.D., Wegmann, K.W., and Scuderi, L.A., 2010, Cracks in desert pavement rocks: Further insights into mechanical weathering by directional insolation: *Geomorphology*, v. 123, p. 97–108, doi:10.1016/j.geomorph.2010.07.003.
- Frankel, K.L., and Dolan, J.F., 2007, Characterizing arid region alluvial fan surface roughness with airborne laser swath mapping digital topographic data: *Journal of Geophysical Research*, v. 112, F02025, doi:10.1029/2006JF000644.
- Gilbert, L.E., 1989, Are topographic data sets fractal?: *Pure and Applied Geophysics*, v. 131, p. 241–254, doi:10.1007/BF00874489.
- Larsen, I.J., Almond, P.C., Eger, A., Stone, J.O., Montgomery, D.R., and Malcolm, B., 2014, Rapid soil production and weathering rates in the Southern Alps, New Zealand: *Science*, v. 343, p. 637–640, doi:10.1126/science.1244908.
- Matmon, A., Simhai, O., Amit, R., Haviv, I., Porat, N., McDonald, E., Benedetti, K., and Finkel, R., 2009, Desert pavement-coated surfaces in extreme deserts present the longest-lived landforms on Earth: *Geological Society of America Bulletin*, v. 121, p. 688–697, doi:10.1130/B26422.1.
- McCarroll, D., and Nesje, A., 1996, Rock surface roughness as an indicator of degree of rock surface weathering: *Earth Surface Processes and Landforms*, v. 21, p. 963–977, doi:10.1002/(SICI)1096-9837(199610)21:10<963:AID-ESP643>3.0.CO;2-J.
- McFadden, L.D., Wells, S.G., and Jercinovic, M.J., 1987, Influences of eolian and pedogenic processes on the evolution and origin of desert pavements: *Geology*, v. 15, p. 504–508, doi:10.1130/0091-7613(1987)15<504:IOEAPP>2.0.CO;2.
- McFadden, L.D., Wells, S.G., and Ritter, J.B., 1989, Use of multiparameter relative-age methods for age determination and correlation of alluvial-fan surfaces on a desert piedmont, eastern Mojave Desert, California: *Quaternary Research*, v. 32, p. 276–290, doi:10.1016/0033-5894(89)90094-X.
- McFadden, L.D., Eppes, M.C., Gillespie, A.R., and Hallet, B., 2005, Physical weathering in arid landscapes due to diurnal variation in the direction of solar heating: *Journal of the Geological Society of America Bulletin*, v. 117, p. 161–173, doi:10.1130/B25508.1.
- Moore, J.E., Pelletier, J.D., and Smith, P.H., 2008, Crack propagation by differential insolation on desert surface clasts: *Geomorphology*, v. 102, p. 472–481, doi:10.1016/j.geomorph.2008.05.012.
- Perfect, E., 1997, Fractal models for the fragmentation of rocks and soils: *Reviews in Engineering Geology*, v. 48, p. 185–198, doi:10.1016/S0013-7952(97)00040-9.
- Perron, J.T., Kirchner, J.W., and Dietrich, W.E., 2008, Spectral signatures of characteristic spatial scales and nonfractal structure in landscapes: *Journal of Geophysical Research*, v. 113, F04003, doi:10.1029/2007JF000866.
- Porat, N., Amit, R., Enzel, Y., Zilberman, E., Avni, Y., Ginat, H., and Gluck, D., 2010, Abandonment ages of alluvial landforms in the hyperarid Negev determined by luminescence dating: *Journal of Arid Environments*, v. 74, p. 861–869, doi:10.1016/j.jaridenv.2009.10.018.
- Portenga, E.W., and Bierman, P.R., 2011, Understanding Earth's eroding surface with <sup>10</sup>Be: *GSA Today*, v. 21, no. 8, p. 4–10, doi:10.1130/G111A.1.
- Quade, J., 2001, Desert pavements and associated rock varnish in the Mojave Desert: How old can they be?: *Geology*, v. 29, p. 855–858, doi:10.1130/0091-7613(2001)029<0855:DPAARV>2.0.CO;2.
- Regmi, N.R., McDonald, E.V., and Bacon, S.N., 2014, Mapping Quaternary alluvial fans in the southwestern United States based on multiparameter surface roughness of lidar topographic data: *Journal of Geophysical Research*, v. 119, p. 12–27, doi:10.1002/2012JF002711.
- Turcotte, D.L., 1997, *Fractals and chaos in geology and geophysics* (second edition): Cambridge, UK, Cambridge University Press, 416 p.
- Weeks, R.J., Smith, M.O., Pak, K., Li, W.-H., Gillespie, A.R., and Gustafson, B., 1996, Surface roughness, radar backscatter and VNIR reflectance in Death Valley, California: *Journal of Geophysical Research*, v. 101, no. E10, p. 23,077–23,090, doi:10.1029/96JE01247.
- Wells, S.G., McFadden, L.D., and Dohrenwend, J.C., 1987, Influence of late Quaternary climatic changes on geomorphic and pedogenic processes on a desert piedmont, eastern Mojave Desert, California: *Quaternary Research*, v. 27, p. 130–146, doi:10.1016/0033-5894(87)90072-X.
- Wells, S.G., McFadden, L.D., Poths, J., and Olinger, C.T., 1995, Cosmogenic <sup>3</sup>He surface-exposure dating of stone pavements: Implications for landscape evolution in deserts: *Geology*, v. 23, p. 613–616, doi:10.1130/0091-7613(1995)023<0613:CHSEDO>2.3.CO;2.
- Yaalon, D.H., 1970, Parallel stone cracking, a weathering process on desert surfaces: *Geological Institute of Bucharest Technology and Economics Bulletin*, v. 18, p. 107–111.

Manuscript received 12 May 2014

Revised manuscript received 8 September 2014

Manuscript accepted 10 September 2014

Printed in USA

## Geology

### Measuring the time and scale-dependency of subaerial rock weathering rates over geologic time scales with ground-based lidar

Amit Mushkin, Amir Sagy, Eran Trabelci, Rivka Amit and Naomi Porat

*Geology* 2014;42;1063-1066  
doi: 10.1130/G35866.1

---

**Email alerting services**

click [www.gsapubs.org/cgi/alerts](http://www.gsapubs.org/cgi/alerts) to receive free e-mail alerts when new articles cite this article

**Subscribe**

click [www.gsapubs.org/subscriptions/](http://www.gsapubs.org/subscriptions/) to subscribe to *Geology*

**Permission request**

click <http://www.geosociety.org/pubs/copyrt.htm#gsa> to contact GSA

Copyright not claimed on content prepared wholly by U.S. government employees within scope of their employment. Individual scientists are hereby granted permission, without fees or further requests to GSA, to use a single figure, a single table, and/or a brief paragraph of text in subsequent works and to make unlimited copies of items in GSA's journals for noncommercial use in classrooms to further education and science. This file may not be posted to any Web site, but authors may post the abstracts only of their articles on their own or their organization's Web site providing the posting includes a reference to the article's full citation. GSA provides this and other forums for the presentation of diverse opinions and positions by scientists worldwide, regardless of their race, citizenship, gender, religion, or political viewpoint. Opinions presented in this publication do not reflect official positions of the Society.

---

**Notes**